

DEVELOPMENT OF INTERNAL PRESSURE MONITORING SYSTEM FOR
CONTROL OF EXPLOSIVE SPALLING IN REFRACTORY CASTABLES

by

DeForrest Lovell Hipps

Thesis submitted to the Faculty of the
Virginia Polytechnic Institute and State University
in partial fulfillment of the requirements for the degree of
MASTER OF SCIENCE
in
Materials Engineering

APPROVED:

J.J. Brown, Jr., Chairman

G.V. Gibbs

D.P.H. Hasselman

October, 1982

Blacksburg, Virginia

DEVELOPMENT OF INTERNAL PRESSURE MONITORING SYSTEM FOR
CONTROL OF EXPLOSIVE SPALLING IN REFRACTORY CASTABLES

by

DeForrest Lovell Hipps

(ABSTRACT)

During the initial heating of hydraulically bonded castable refractories, dehydration of cement phases causes build-up of high levels of internal steam pressure. If this pressure exceeds material strength, explosive spalling results. A probe capable of measuring internal steam pressures "in-situ" has been developed and tested. Correlation of cement calorimetry and pressure data suggests that castable heating schedules can be modified to reduce explosive spalling.

ACKNOWLEDGMENTS

The author wishes to express his sincere appreciation to Prof. J.J. Brown, Jr. for his invaluable advice and criticism during the period of this work. Special thanks go to Rick Keith, Curtis Martin, Larry Slusser, and Dr. Robert Morena for much needed assistance in material acquisition and equipment design. Also, a special note of thanks goes to the members of the Blacksburg martial arts community for their support and good fellowship. Finally, the author would like to thank his parents for all of the encouragement given to him throughout the course of his studies at V.P.I. & S.U.

TABLE OF CONTENTS

	PAGE
ABSTRACT	ii
ACKNOWLEDGMENTS	iii
LIST OF ILLUSTRATIONS	v
I. INTRODUCTION	1
II. LITERATURE SURVEY	2
A. Manufacture of High Alumina Castables	2
B. Cement Curing and Dehydration	3
C. Factors Contributing to Explosive Spalling	6
1. Material Properties	6
2. User Controlled Variables	7
III. INTERNAL PRESSURE MONITORING SYSTEM	12
A. Pressure Probe	12
B. Laboratory System	12
C. Installation	16
IV. EXPERIMENTAL PROCEDURES	17
A. Differential Scanning Calorimetry of Cement Phases	17
B. Internal Pressure Measurement	17
V. EXPERIMENTAL RESULTS	19
A. DSC Measurements	19
B. Internal Pressure Measurements	19
VI. DISCUSSION	29
A. Performance of Probe System	29
B. Conclusions Based Upon Internal Pressure Measurement	30
1. Water Vapor Generation	30
2. Internal Steam Pressure Intensities	30
3. Factors Leading to Explosive Spalling	32
VII. CONCLUSIONS	34
VIII. RECOMMENDATIONS	35
IX. LITERATURE SOURCES	36
VITA	38

LIST OF ILLUSTRATIONS

<u>Figures</u>		<u>Page</u>
1	Steam Volumes Produced During Dehydration of Calcium Aluminate Cements	8
2	Internal Pressure Probe	13
3	Internal Pressure Monitoring System . . .	14
4	DSC of Hydrated Cement Phases	20
5	Comparison of Specimen Which Explosively Spalled at 1700°F With Unfired, As-Cast Specimen	21
6	Internal Pressure vs. Temperature Using 1000°F Hot Face	22
7	Internal Pressure vs. Temperature Using 1700°F Hot Face	24
8	Heat-Up Rates of Probes at Various Depths From 1000 and 1700°F Hot Faces	27
9	Maximum Steam Pressures Measured at Various Depths from 1000 and 1700°F Hot Face	28
10	In-Pore Steam Pressure vs. Radius of Dehydrating Spherical Volume of Castable Having 10% Bulk Porosity	31
<u>Table</u>		
1	Reactions Involving Aluminous Cement Phases	4

I. INTRODUCTION

High alumina castables have gained widespread use in the refractories industry over the past two decades. The dehydration reactions that occur during initial heating of castables generate large volumes of water vapor. If these vapors are created faster than they can be relieved through the pores of the material, internal pressures will build and explosive spalling will occur (17). A system that monitors internal steam pressures can prevent explosive spalling and refractory failure.

The purpose of this investigation is to 1) develop a device that will measure internal steam pressures generated within a castable lining during initial heat-up and 2) to demonstrate the feasibility of measuring internal steam pressures in commercial installations.

The probe developed in this study is based on a strain gauge pressure transducer. Vapor pressure is measured through a stainless steel tube cast into the refractory wall. The probe is attached to the tube and then to recording equipment or furnace heating controls.

II. LITERATURE SURVEY

A. Manufacture of High Alumina Castables

High alumina cements are manufactured by the fusion of high-purity limestone and bauxite. This product is rapidly quenched, then ground to -200 mesh. Principal phases are CA, CA₂, and A*. Also present in minor amounts is C₄AF which results from the addition of F as a flux to aid in the fusion of the raw materials (14). On the average, alumina cements contain less than 20 wt.% impurities (5).

Concrete properties are determined to a large extent by the attention given the material during the mixing and curing stages. Water content is important; too little water produces insufficient compaction (15), whereas excess water promotes particle segregation and low strength (3). It has been recommended that a cement to water ratio of 1.75 yields optimum results (7). In order to assure complete hydration of the castable, including the surface layers, curing time should be greater than 20 hours under at least 95% relative humidity (16). Curing at 77°F or higher is necessary for maximum strength development (15).

*Cement notation: A=Al₂O₃, C=CaO, F=Fe₂O₃, H=H₂O, S=SiO₂.

B. Cement Curing and Dehydration

Extensive research has been conducted on the curing and dehydration of calcium aluminate cements. Reactions that occur during initial heating are summarized in Table 1. Major phases encountered are CAH_{10} , C_2AH_8 , C_3AH_6 , $\text{C}_4\text{A}_3\text{H}_3$, CH , and AH_3 .

CAH_{10} occurs as hexagonal prisms and is the primary hydrate formed at room temperature or below. Above 70°F , CAH_{10} dehydrates to C_2AH_8 and AH_3 with 3 molecules of water being evolved (1,6). At least one reference reports that this reaction occurs at 95°F (9).

The hexagonal phase C_2AH_8 exists as a metastable intermediate phase in the transition of CAH_{10} to more stable hydrates. C_2AH_8 dehydrates at 129°F to form C_3AH_6 and AH_3 .

The cubic hydrate C_3AH_6 is the dominant phase at cure temperatures greater than 145°F . This phase dehydrates in two stages (8,13). The first stage involves the loss of 4.5 molecules of water at 527°F , yielding the metastable phase $\text{C}_3\text{AH}_{1.5}$. The second stage occurs at 1022°F where C and C_{12}A_7 are produced. At 437°F in a water saturated atmosphere, C_3AH_6 converts to $\text{C}_4\text{A}_3\text{H}_3$, CH , and H . One source states that C_3AH_6 is only stable to 419°F (11).

TABLE 1
Reactions Involving Aluminous Cement Phases

Temperature (°F)	Reaction	Reference
70-72	$2\text{CAH}_{10} \Rightarrow \text{C}_2\text{AH}_8 + \text{AH}_3 + 9\text{H}$	1, 6, 13
95	$2\text{CaH}_{10} \Rightarrow \text{C}_2\text{AH}_8 + \text{AH}_3 + 9\text{H}$	9
129	$3\text{C}_2\text{AH}_8 \Rightarrow 2\text{C}_3\text{AH}_6 + \text{AH}_3 + 9\text{H}$	6
302	$\text{AH}_3(\text{Gibbsite}) = \text{AH}(\text{Boehmite}) + 2\text{H}$	11
419	$7\text{C}_3\text{AH}_6 \Rightarrow 9\text{C} + \text{C}_{12}\text{A}_7 + 42\text{H}$	11
437	$3\text{C}_3\text{AH}_6 \Rightarrow \text{C}_4\text{A}_3\text{H}_3 + 5\text{CH} + 10\text{H}$	8
446	$7\text{C}_3\text{AH}_6 \Rightarrow \text{C}_{12}\text{A}_7 + 9\text{CH} + \text{AH}_3 + 33\text{H}$	10
527	$\text{C}_3\text{AH}_6 \Rightarrow \text{C}_3\text{AH}_{1.5} + 4.5\text{H}$	8, 13
572	$\text{AH} \Rightarrow \text{gamma-A} + \text{amorphous-A} + \text{H}$	8, 13
752	$\text{CH} \Rightarrow \text{C} + \text{H}$	10
1022	$7\text{C}_3\text{AH}_{1.5} \Rightarrow 9\text{C} + \text{C}_{12}\text{A}_7 + 10.5\text{H}$	8, 13
1328-1382	$17\text{C}_4\text{A}_3\text{H}_3 \Rightarrow 5\text{C}_{12}\text{A}_7 + 8\text{CA}_2 + 51\text{H}$	13

$C_4A_3H_3$ is an unstable orthorhombic phase which dehydrates at 1328-1382°F to form $C_{12}A_7$ and CA_2 .

The calcium hydrate, CH, is formed by hydrothermal decomposition of C_3AH_6 at 446°F. CH is a stable phase which dehydrates at 752°F to form C and water.

AH_3 (Gibbsite) is the stable aluminum hydrate over the temperature range 77 to 300°F. At curing temperatures less than 77°F a metastable alumina gel is formed. This gel is known to reduce the apparent porosity of the concrete and contribute to explosive spalling (6). Alumina gel readily crystallizes to form Gibbsite with increasing temperature or moderate aging. Gibbsite dehydrates at 302°F to form AH (Boehmite). At 572°F, Boehmite decomposes to form gamma and amorphous A.

DTA studies of CA cement dehydration indicate a great deal of variability of reaction temperature (12). For the hydrate CAH_{10} , stepwise dehydration at 311 and 545°F is recorded. C_3AH_6 shows the first stage dehydration at 644°F and the second at 1022°F. AH (Boehmite) dehydrates at 626°F to gamma-A which later transforms to alpha-A.

C. Factors Contributing to Explosive Spalling

1. Materials Properties

Material properties influencing explosive spalling include castable permeability and cement bond strength (4,17). Other factors include particle size distribution and the relative amounts of cement and aggregate.

Castable permeability directly controls explosive spalling resistance. Steam pressure generated within the castable must be allowed to rapidly diffuse to the surface or explosive spalling will result. If castable permeability is low, or many of the pores are isolated, steam pressure will build until material failure occurs.

To resist explosive spalling, the cement bond must also have maximum strength. The formation of large crystals or high density phases in the cement during curing reduces the bonding surface area between aggregate and cement and creates intergranular voids. The reduction of surface area of the cement grains and formation of voids seriously reduces the strength of the final product.

Particle size distributions of cement and aggregate must be regulated to maximize strength and minimize void formation. Use of large aggregate particles promotes void

formation due to incomplete compaction. Strength is also sacrificed because bonding surface to volume ratios of grains are less. However, mixes favoring fine particles create very dense castables with low permeability.

Cement content also influences resistance to explosive spalling. Too little cement results in higher porosity, insufficient bonding, and lowered strength. The amount of water required to insure workability of concretes with large cement to aggregate ratios is very high. Any excess pore water leads to dangerous pressure build-up during initial heating.

2. User Controlled Variables

Resistance of castables to explosive spalling is largely determined by concentration of casting water, castable thickness, method of placement (casting, gunning, or ramming), curing temperature, and heat-up rates.

During the mixing stage, only 1/4 of total casting water is "combined" as part of hydraulic bonding. The remainder is locked in pores and is available for conversion to steam at 212°F. This pore water forms the primary source for vapor generation in the castable lining. Figure 1 shows the relative volumes of steam produced by dehydration reactions during initial firing. Calculations

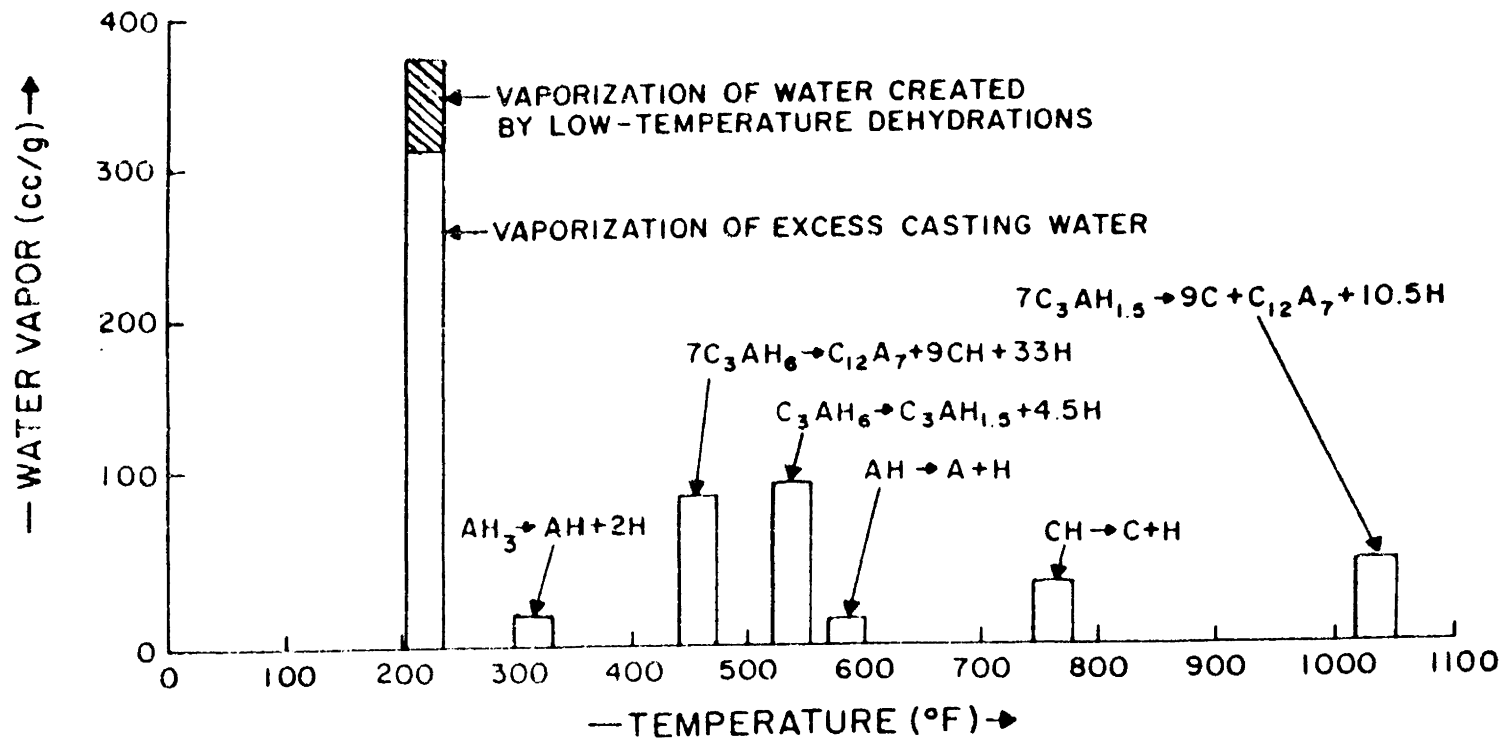


Fig. 1. Steam volumes produced during dehydration of calcium aluminate cements.

are based on a concrete mix using 10 g of dry cement, a water to cement ratio of 0.4, and hydrate phases produced by curing at 72°F (6).

Castable thickness greatly influences resistance to explosive spalling. Because steam dissipation is slower in thick sections, initial heat up must be done carefully to prevent failure.

The method of castable installation also affects spalling characteristics. Cast concretes typically have lower porosity than gunned or rammed mixes. Permeability is also lower because pores tend to be isolated rather than connected. In gunned or rammed concretes, the pore structure tends to be more open since mixes must be drier to assure workability. Less efficient compaction results in void formation and allows more rapid steam pressure dissipation. Explosive spalling is aggravated by cosmetic "slicking" of the gunned surface which closes many pores (2).

The importance of room temperature curing is shown by Gitzen and Hart in a 1961 study (4). In this experiment, 2.5" tabular alumina castable cubes consisting of 15 wt.% CA-25 cement were cured at different temperatures. These samples were then fired at successively higher temperatures

until explosive spalling occurred. Curing temperatures and temperatures at which explosive spalling occurred are shown below.

T(°F) CURING	T(°F) EXPLOSION
40	1120
50	1240
60	1530
70	2050
80	2760
90,100,110	>3000

As can be seen from the data, resistance to explosive spalling decreases rapidly with curing temperatures below 60°F.

For cements cured at low temperatures, the primary hydrates formed are CAH_{10} and alumina gel, AH_x . The amorphous gel, AH_x has a large specific surface. This large specific surface bonds grains tightly and lowers permeability. Also the water to mass ratios of both hydrate molecules are much higher than those of phases formed at higher curing temperatures. The high water content of the cement phases makes high temperature dehydration reactions more violent, increasing the risk of explosive spalling.

To allow internal vapor pressure to dissipate, heat up rates must be moderate during initial firing. In order to

prevent explosive spalling, a rate no faster than 100-200°F/hr is recommended (2).

With different concrete compositions and installation procedures the susceptibility of castables to explosive spalling is highly variable. Therefore, a probe that constantly measures changing internal steam pressures is extremely desirable.

III. INTERNAL PRESSURE MONITORING SYSTEM

A. Pressure Probe

To measure the steam pressures generated within a large castable wall "in-situ", a probe incorporating a transducer was developed (see Figure 2). This probe incorporates a strain gauge pressure transducer to give instantaneous measurement of pressure fluctuations. To protect the diaphragm of the transducer from high-temperature steam, the transducer is attached to a 1/4" O.D. SS tube which is partially filled with silicone diffusion pump oil. The length of tube filled with oil acts as a thermal baffle, allowing the dissipation of heat by radiation. A Nichrome-wrapped Pyrex heating coil prevents pressure loss from steam condensation by heating the surface of the oil to 300°F. A Pyrex spacing ring separates the heating coil and transducer.

B. Laboratory System

For laboratory-scale research, a two channel internal pressure monitoring system was constructed (see Figure 3). The test sample size used was 7x9x6". The bottom of the sample mold forms the test hot face and the 2 probe tubes are cast through the mold top. The two probes attached to each sample use SS tubes cast at 1/2" intervals

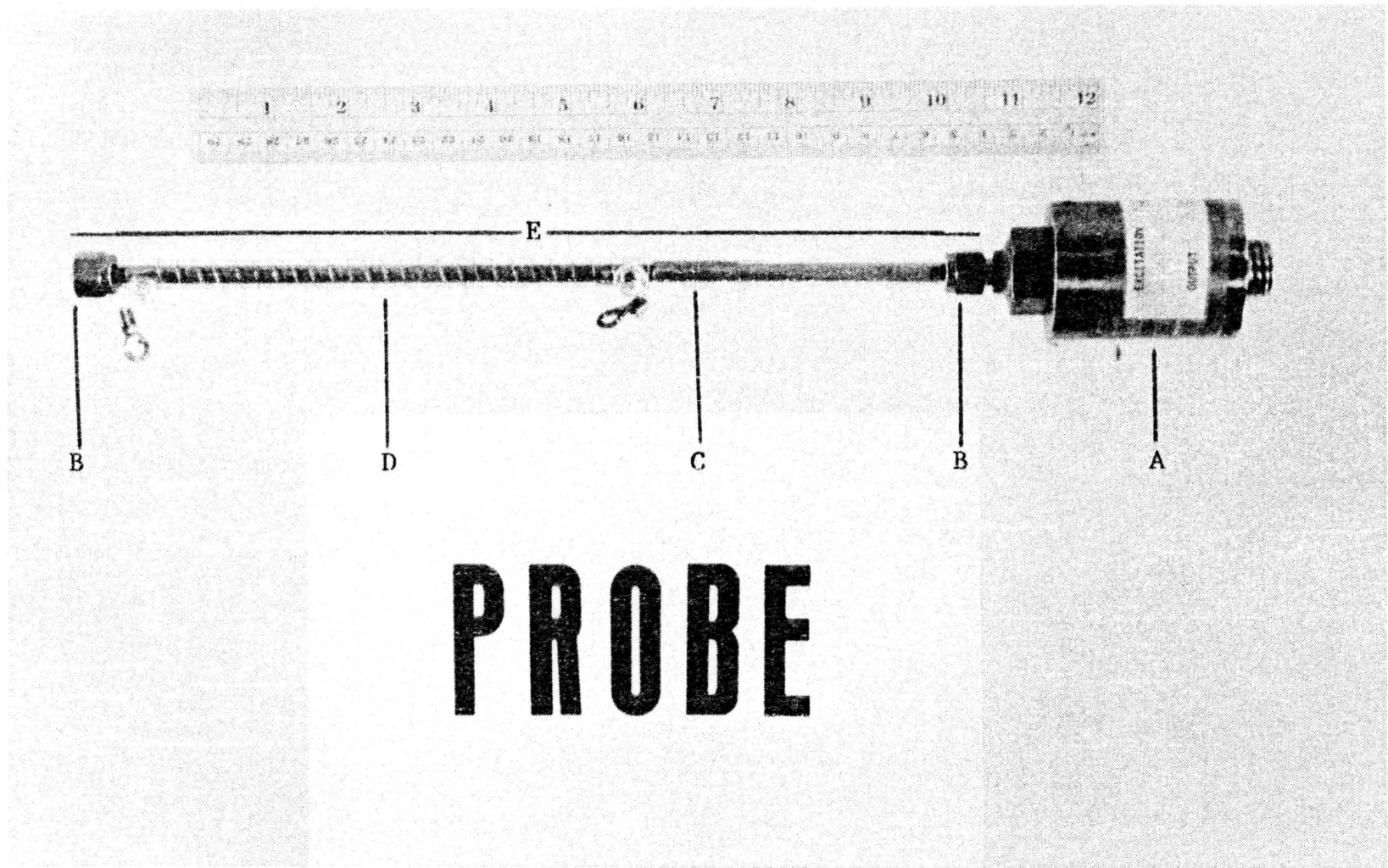


Fig. 2. Internal pressure probe.

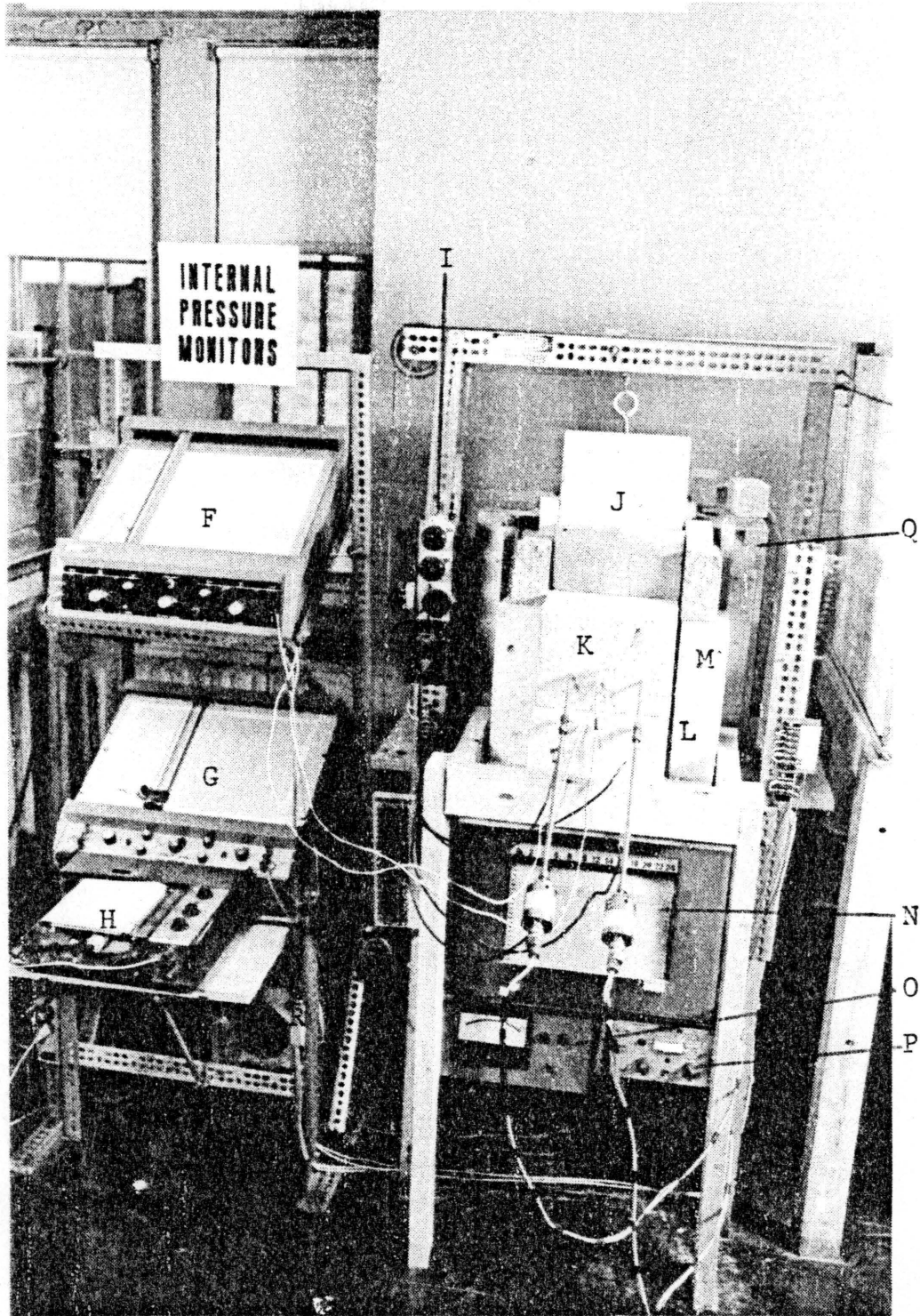


Fig. 3. Internal pressure monitoring system.

INDEX AND VENDOR'S LIST FOR FIGURES 2 & 3

- A. Series 152 Gauge Pressure Transducer: MB/ALINCO, MB ELECTRONICS
- B. SS Tube Fittings: SWAGELOCK
- C. Pyrex Spacing Ring: **
- D. Nichrome/PYREX Heating Coil: **
- E. 1/4" O.D. SS Tube
- F. X-Y Plotter: VARIAN ASSOCIATES
- G. X-Y Plotter: MFE
- H. Strip Chart Recorder: BAUSCH & LOMB INC.
- I. Warning Lights: **
- J. Guillotine - Style Furnace Door: **
- K. Castable Block: **, Calcined Kaolin - CE MINERALS, Kyanite - VIRGINIA KYANITE, Calcium Aluminate Cement - ALCOA CA-25C
- L. Pressure Probes: **
- M. Type K Thermocouples: **
- N. 20 Channel Thermocouple Recorder - HONEYWELL
- O. Furnace Controller
- P. Transducer Power Supply - POWER DESIGNS
- Q. Furnace - THERMOLYNE
- R. VARIAC Heating Coil Power Supply

** Fabricated on site.

back from the hot face. A small furnace modified with a guillotine-style sliding door was used to simulate rapid heating rates by enabling one face of a sample to be inserted into a preheated environment. Two X-Y recorders record data on pressure-temperature graphs. Also included in the system is a transducer power supply, furnace controller, and a heating coil power supply. A 20 channel thermocouple recorder is included in the laboratory system to measure heat up rates in test specimens.

C. Installation

In the field, a 1/4" O.D. SS tube is cast into the refractory lining to the depth of interest. This tube is cast at an angle sloping down and away from the hot face. The end of the tube within the furnace is coated with a thin film of paraffin wax to prevent infiltration of cement during the gunning process. At the same depth as the SS tube, Type K thermocouples are cast in order to provide a temperature reference. The probe is then attached to the end of the tube outside the furnace shell. Outputs from the transducers and thermocouples are recorded on strip charts and correlated to give pressure vs. temperature and temperature vs. time plots.

IV. EXPERIMENTAL PROCEDURES

A. Differential Scanning Calorimetry of Cement Phases

DSC measurements were conducted on hydrated cements over the range of 70 to 1050°F. Dehydration and phase change temperatures were then determined from DSC data.

B. Internal Pressure Measurement

Raw materials used in this study consisted of calcined kaolinite (75 wt.%), calcined kyanite (5 wt.%), and CA-25C high alumina cement (20 wt.%). These materials were mixed to ball-in-hand consistency¹ then cast in an aluminum mold. Samples were then cured at room temperature for 24 hours at 100% relative humidity.

Two profiles of pressure and temperature vs. depth were constructed using hot face temperatures of 1000 and 1700°F. For each profile, 8 samples were tested. Each sample had 2 probes cast at different depths. From these tests, internal pressure vs. temperature curves were derived at 1/2" intervals from 0-4" back from the hot face. With each depth of measurement, instrument volumes varied with probe length. By converting the internal volumes of

¹ASTM recommended practice.

each probe to a standard ($P_{\text{recorded}} \times V_{\text{instrument}} = P_{\text{corrected}} \times V_{\text{standard}}$), pressure readings were corrected to allow direct data comparison. Also, heating rate curves were generated from time base measurements of temperature.

V. EXPERIMENTAL RESULTS

A. DSC Measurements

Dehydration reaction temperatures observed by analysis of DSC measurement of cement phase dry-out compare well with literature values (see Figure 4). Dehydration begins at room temperature and continues until approximately 900°F. Because events are so closely spaced, some are observable only as curve inflections rather than sharp endotherms.

B. Internal Pressure Measurement

Sheet-like spalling of castable materials occurred in all specimens tested at 1700°F. All spalled specimens lost layers of uniform 1/2" thickness (see Figure 5). Samples that spalled repeatedly lost layers of 1/2" with each explosion. Explosions were extremely violent and occurred within a matter of seconds after sample insertion into the furnace.

Profiles of pressure and temperature vs. as-cast depth for hot face temperatures of 1000 and 1700°F are shown in Figures 6-7. The original data as recorded on the X-Y recorders were in units of millivolts on both axis. These readings were converted to pressure and temperature values according to transducer and thermocouple manufacturer conversion formulae.

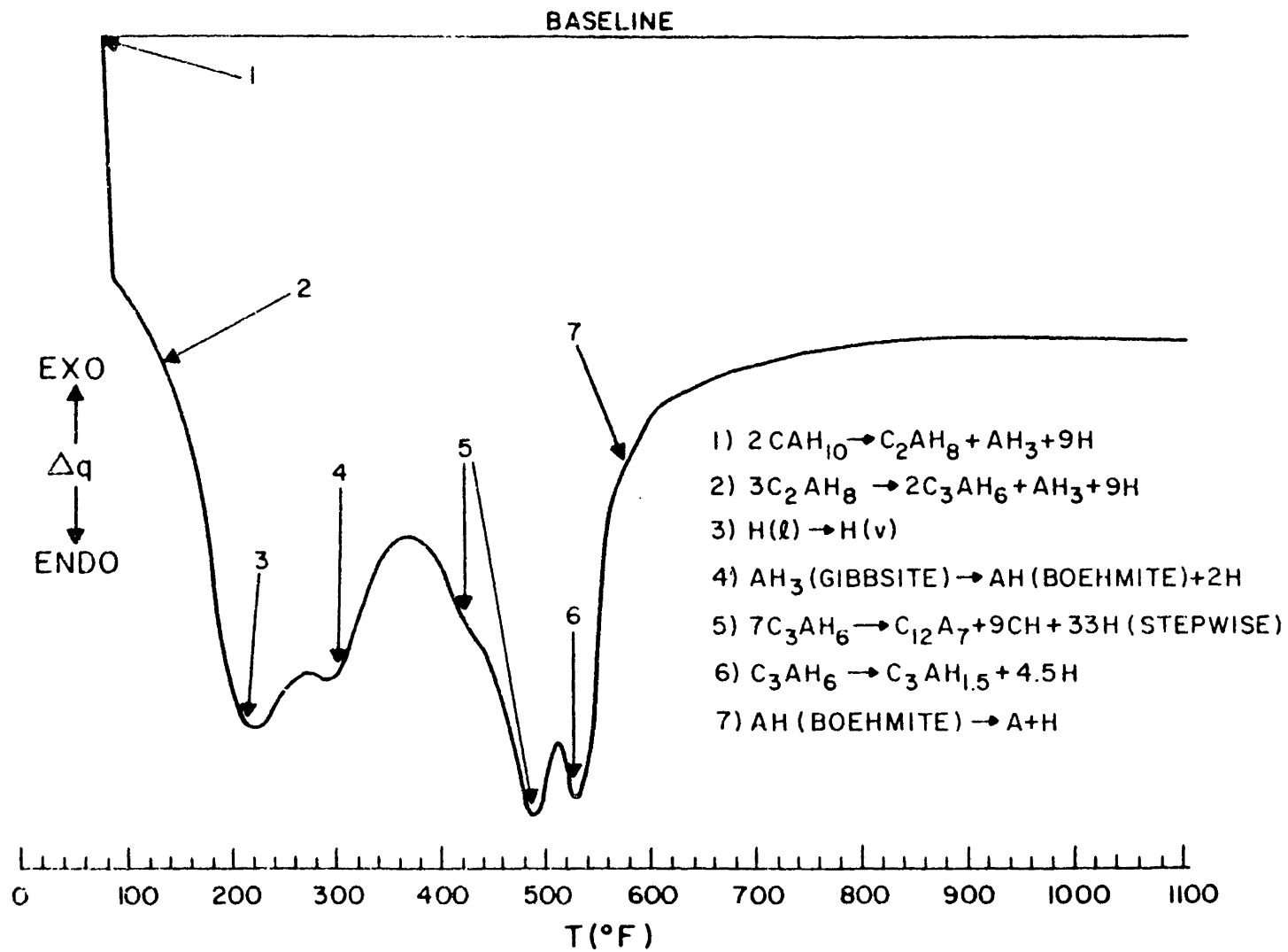


Fig. 4. DSC of hydrated cement phases.

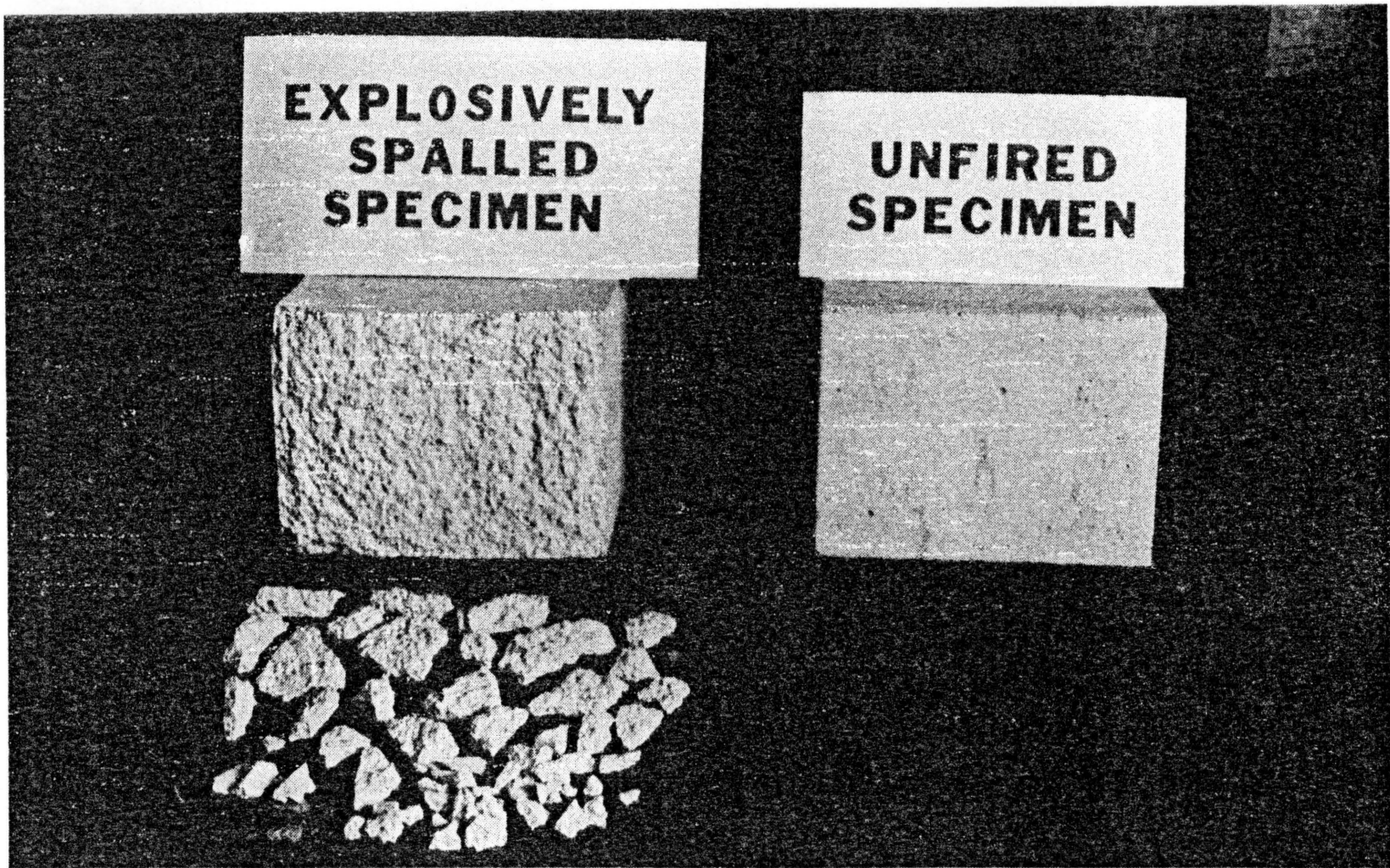


Fig. 5. Comparison of specimen which explosively spalled at 1700°F (left) with unfired, as-cast specimen (right).

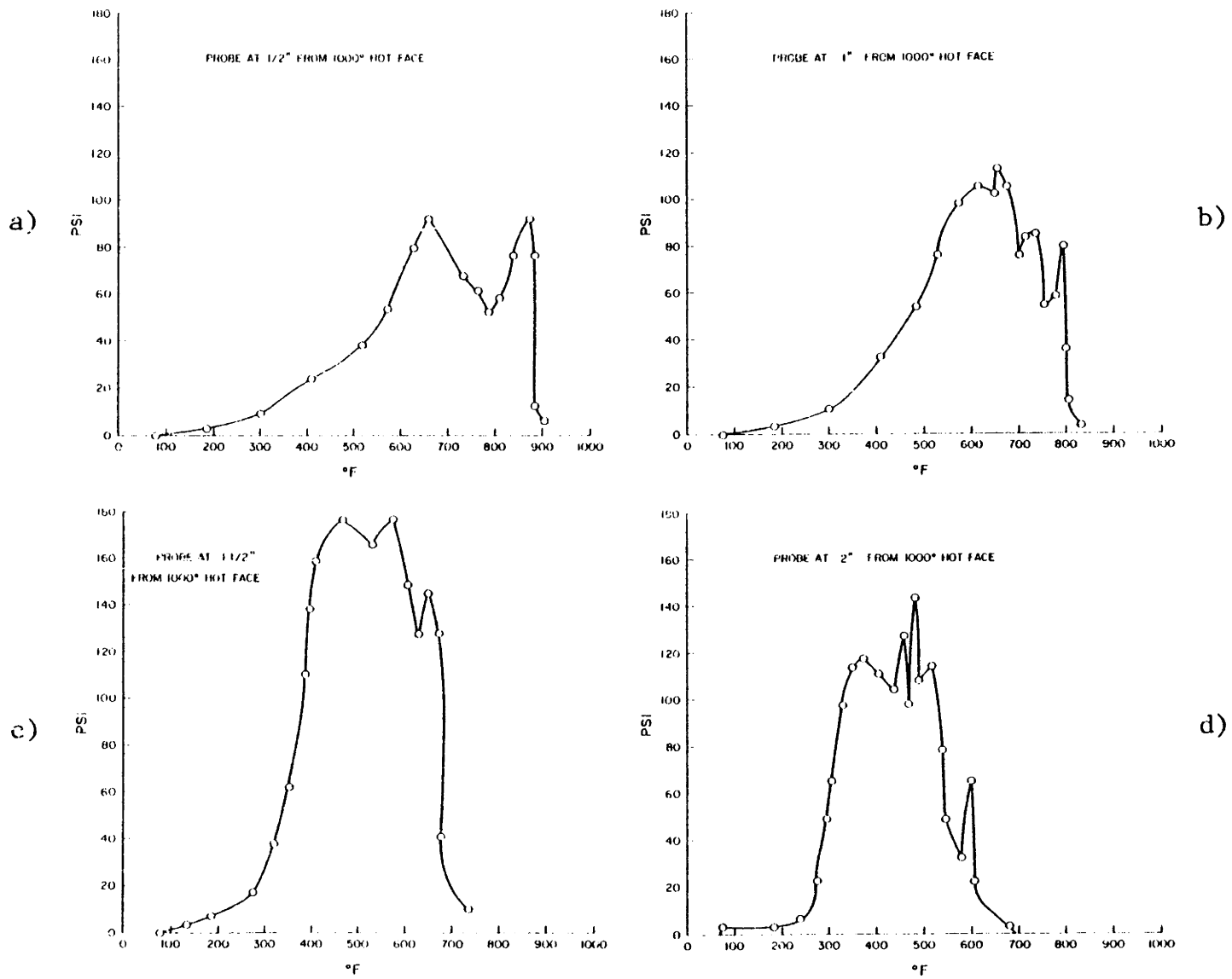


Fig. 6. Internal pressure vs. temperature using 1000°F hot face.

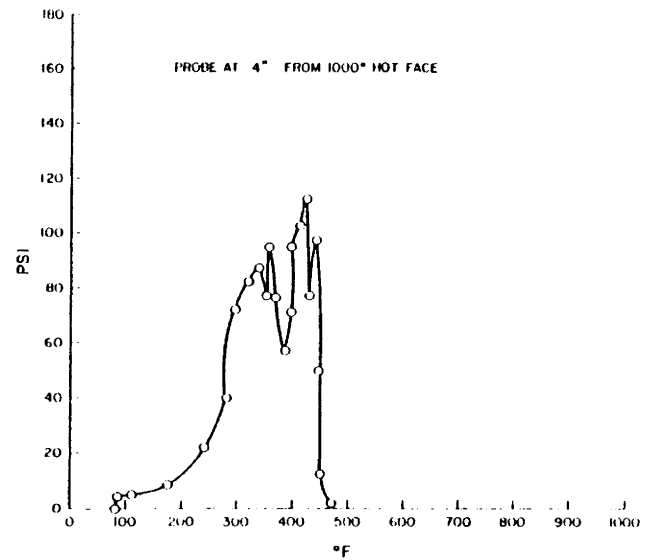
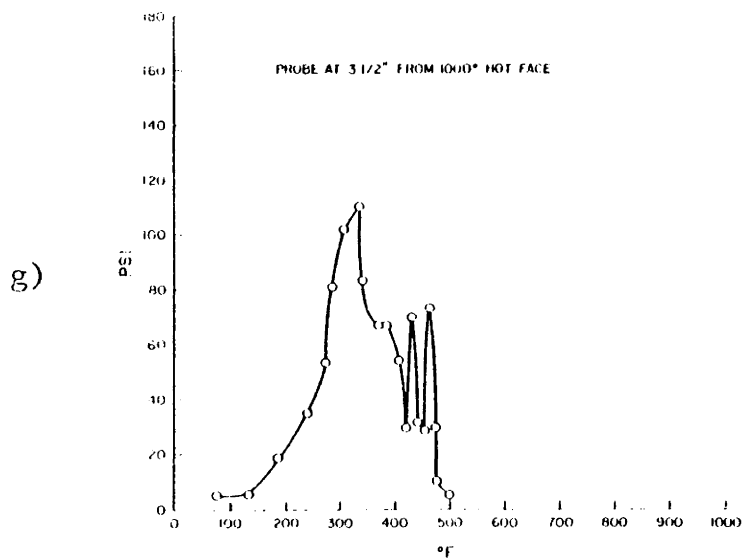
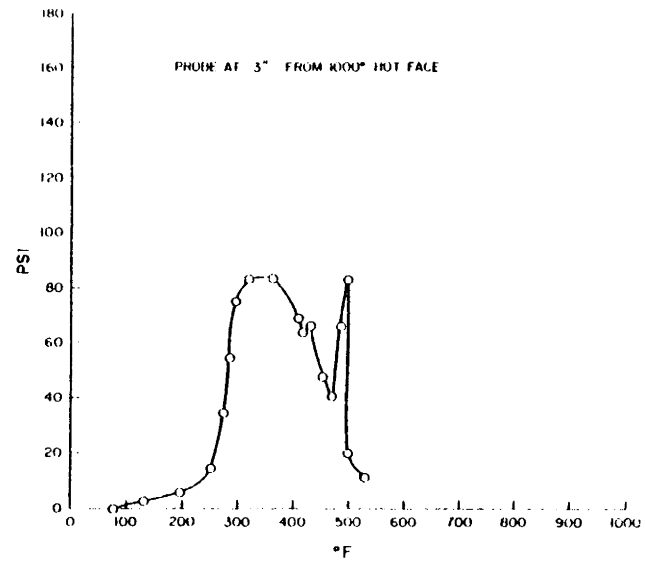
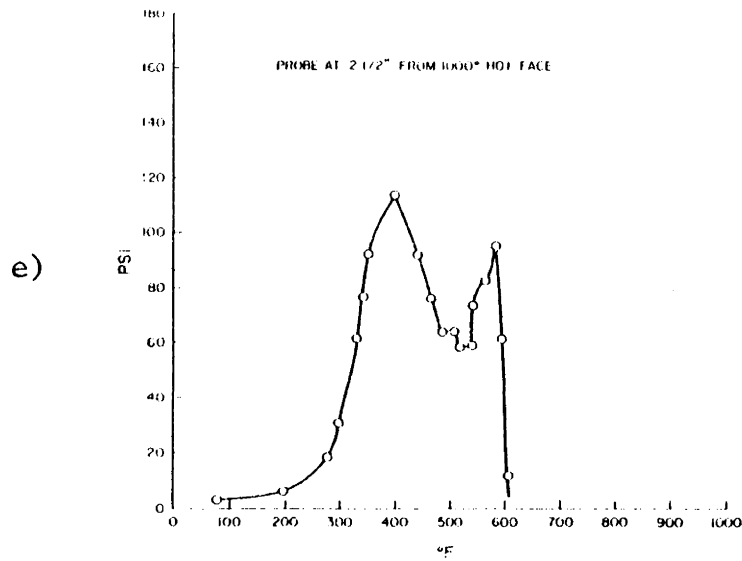


Fig. 6. (Cont'd)

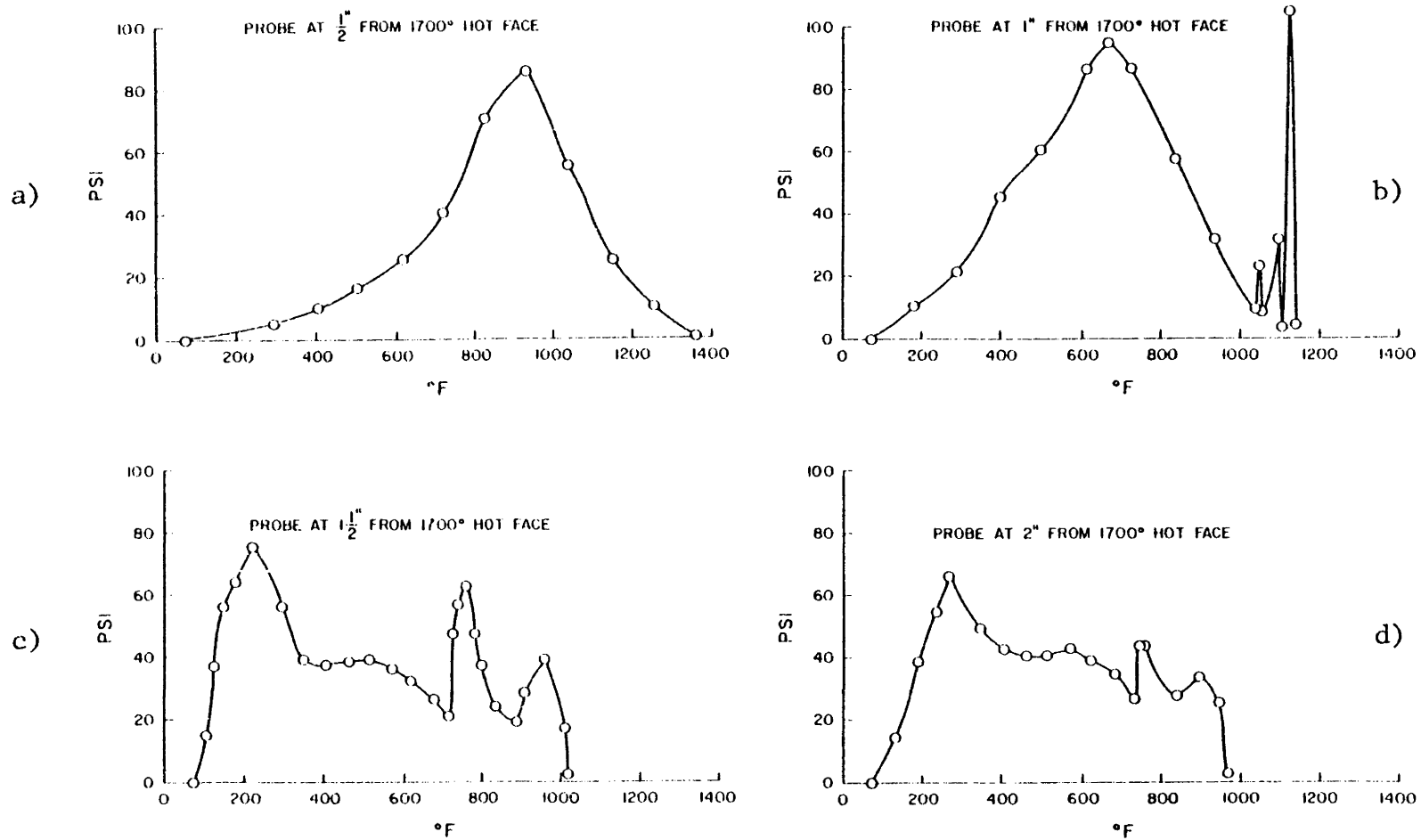


Fig. 7. Internal pressure vs. temperature using 1700°F hot face.

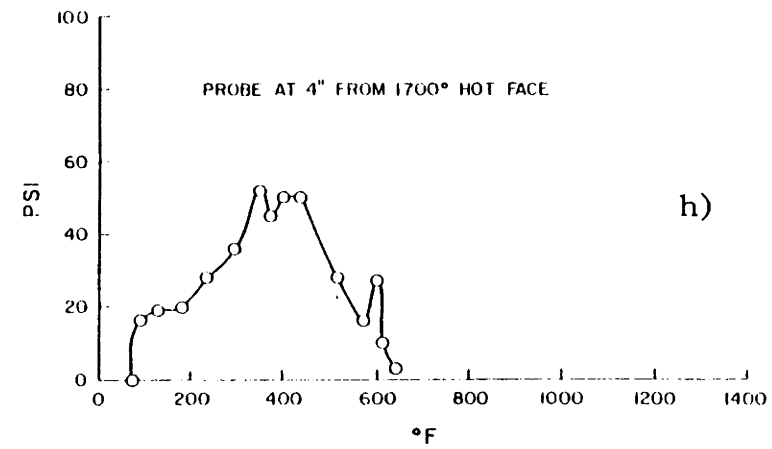
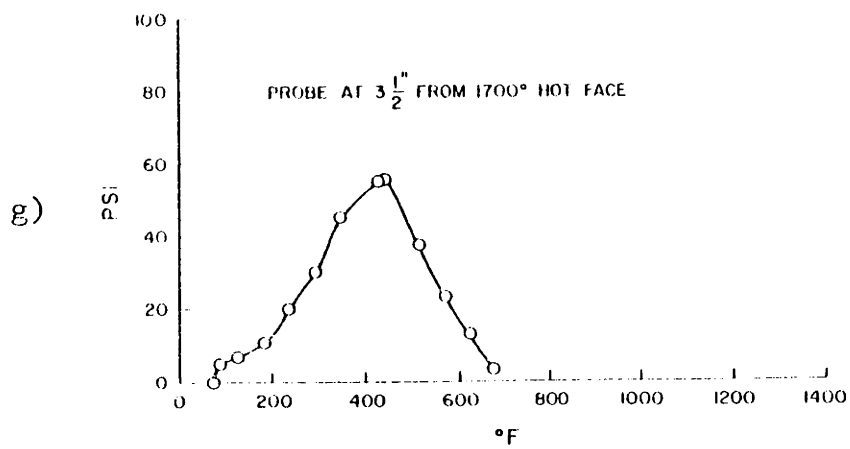
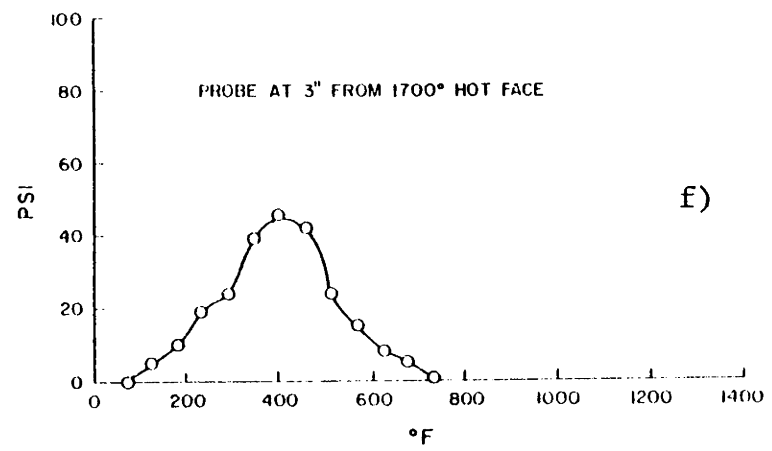
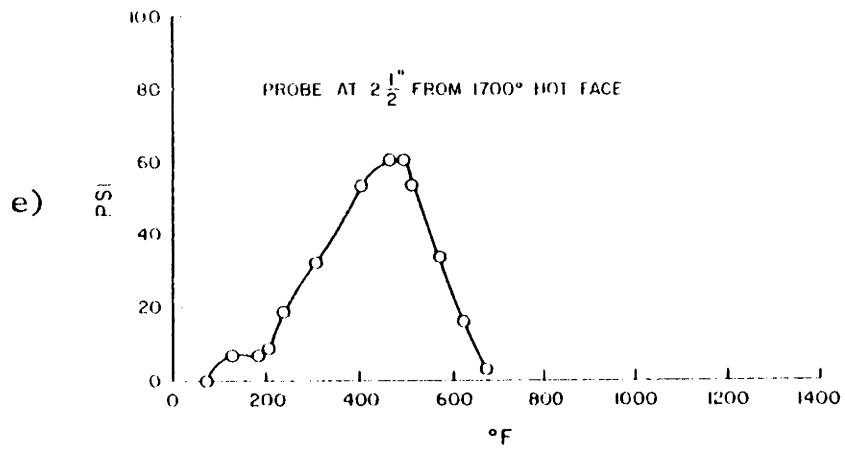


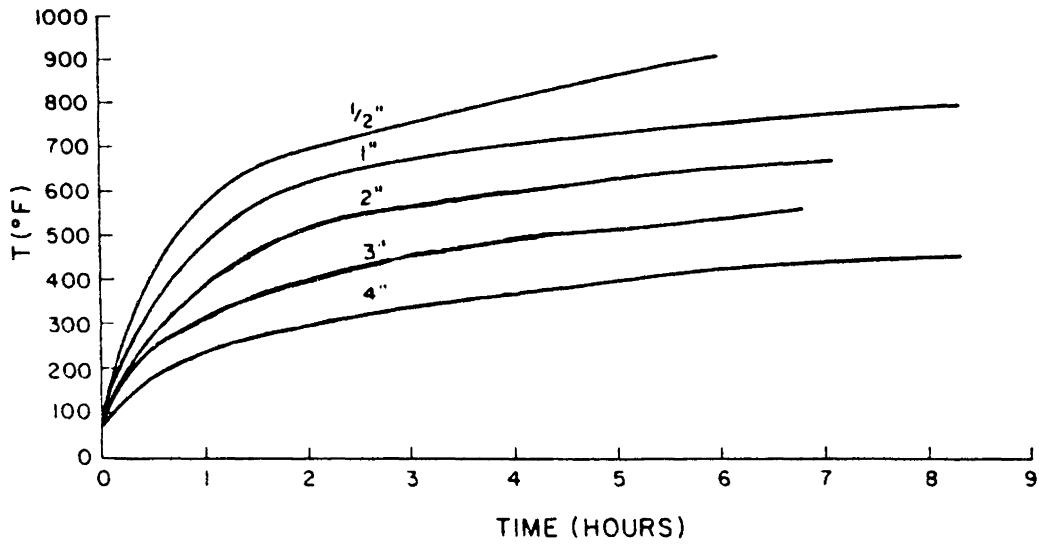
Fig. 7. (Cont'd)

Heating rate curves for hot face temperatures of 1000 and 1700°F are shown in Figure 8. Initial heat-up for both hot face temperatures is quite rapid. From time of sample insertion, heating rates decrease until final temperatures are reached.

A plot of internal pressure maxima vs. depth from a 1000°F hot face was constructed (see Figure 9a). A 180 psig (12.4 MPa) maximum exists at 1 1/2" after which pressure decreases linearly to 80 psig (5.5 MPa) at 3". An increase to 110 psig (7.58 MPa) follows and stays level at greater depths from the hot face.

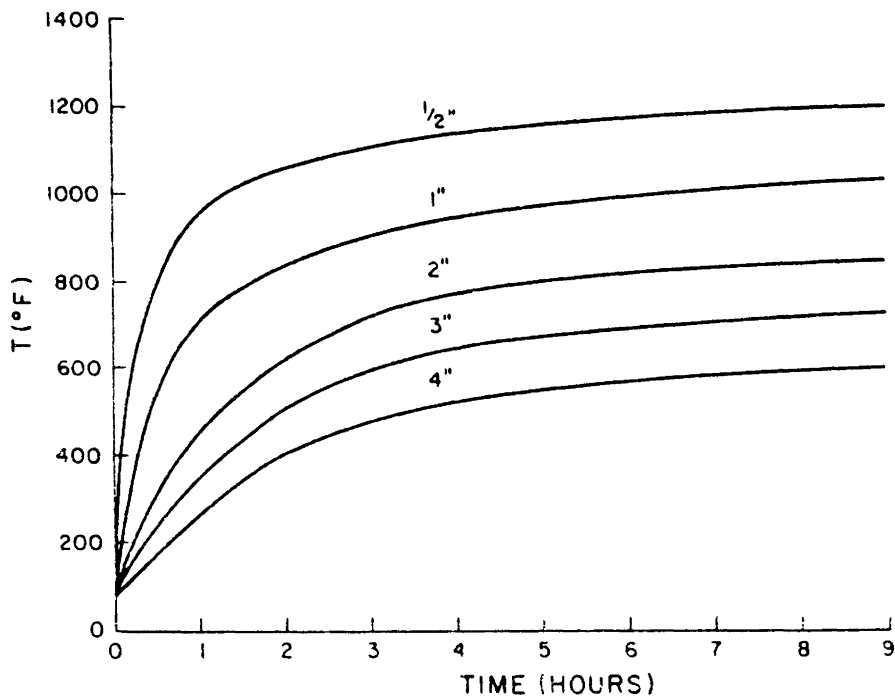
A similar plot for a 1700°F hot face shows a 105 psig (7.24 MPa) maximum at 1" (Figure 9b). At depths further from the hot face, internal pressure maxima decrease to 43 psig (2.96 MPa) at 3" then increase slightly at greater depths. It should be noted that explosive spalling of the hot face was very rapid and occurred before any pressure build up at probe depths was recorded.

Internal pressure maxima using a 1700°F hot face are lower than those using a 1000°F hot face for two reasons. First, at 1700°F the relatively impermeable hot face in all specimens was blown off. This exposed more pores to the surface and allowed steam to dissipate more rapidly. Second, with failure of the hot face, the entire specimen experienced microcracking. These cracks vented steam pressure directly to the surface.



HEAT-UP RATES OF PROBES AT VARIOUS DEPTHS FROM A 1000° HOT FACE

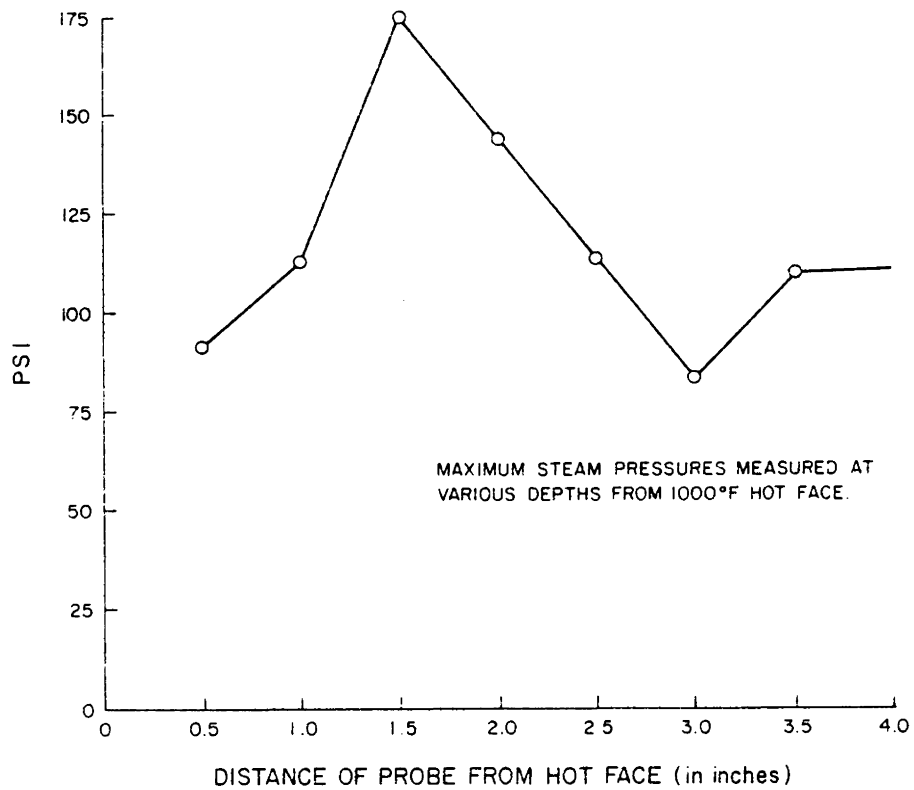
(a)



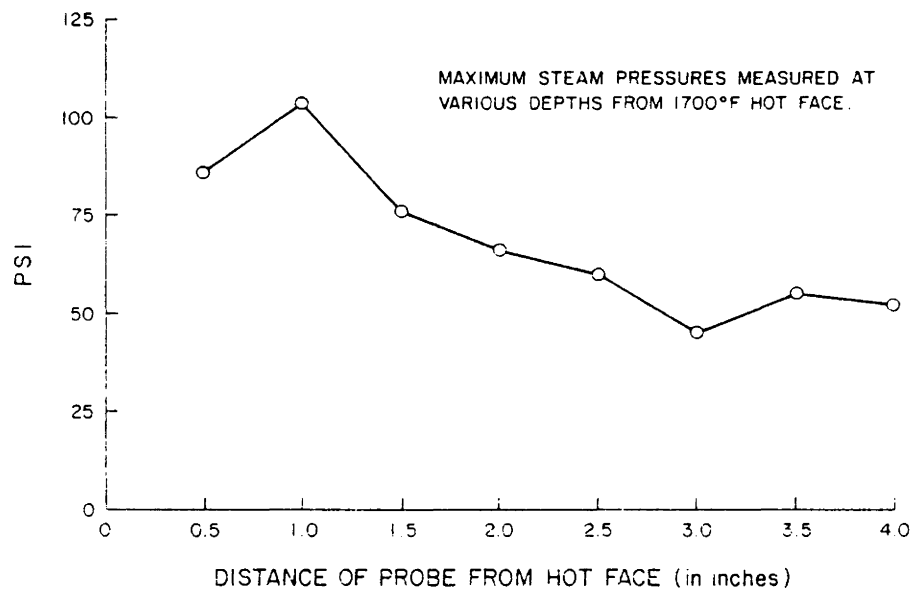
HEAT-UP RATES OF PROBES AT VARIOUS DEPTHS FROM A 1700°F HOT FACE

(b)

Fig. 8



(a)



(b)

Fig. 9

VI. DISCUSSION

A. Performance of Probe System

The probe system is simple to install, easily compatible with most types of on-site recording equipment, and very reliable.

The probe itself is compact, giving it a good life expectancy when installed in exposed areas. Each probe requires only one tubing and six electrical connections. Use of multiplug connectors makes installation very simple and requires only a minimum of equipment.

The voltage output from the pressure probe, when installed on site, may be recorded on thermocouple recorders as degrees of temperature, converted back to millivolts, then to pressure units according to specifications of the pressure transducer. Connections are made to the probe as are thermocouple connections. This allows the use of existing recording equipment normally used during furnace operation.

Measurements made with the pressure probe show excellent repeatability in redundant testing. System stability is good, no adjustments being necessary once measurement begins.

B. Conclusions Based Upon Internal Pressure Measurement

1. Water Vapor Generation

Correlation of DSC data and pressure probe output indicates that the primary events contributing to water vapor generation in order of importance are 1) the vaporization of interstitial water at 212°F, 2) the dehydration of C_3AH_6 at 445 and 525°F, 3) the dehydration of $C_3AH_{1.5}$ at 1022°F and 4) the decomposition of CH at 750°F. The pressure effect of casting water is dependent upon the time between curing and initial firing. If castables are allowed to dry sufficiently before heat-up, only the higher temperature dehydrations will be of importance.

2. Internal Steam Pressure Intensities

Intensities measured by the internal pressure probe are good references for comparison but are much lower than those found within actual pores. Because the pressure dissipates through a large instrument volume the actual "in-pore" pressure may be magnitudes higher. Figure 10 shows theoretical levels of in-pore steam pressure. Assumptions are made as follows:

1. The volume of castable contributing steam to the pressure probe is a sphere of radius r .
2. The pressure probe tube lies at the center of the dehydrating sphere.
3. Castable porosity is constant at 10%.
4. Pores are interconnected within the sphere.
5. Steam generated within the sphere dissipates only through the pressure probe, not the sphere wall.
6. The pressure probe is recording pressure at 100 psig (6.89 MPa).

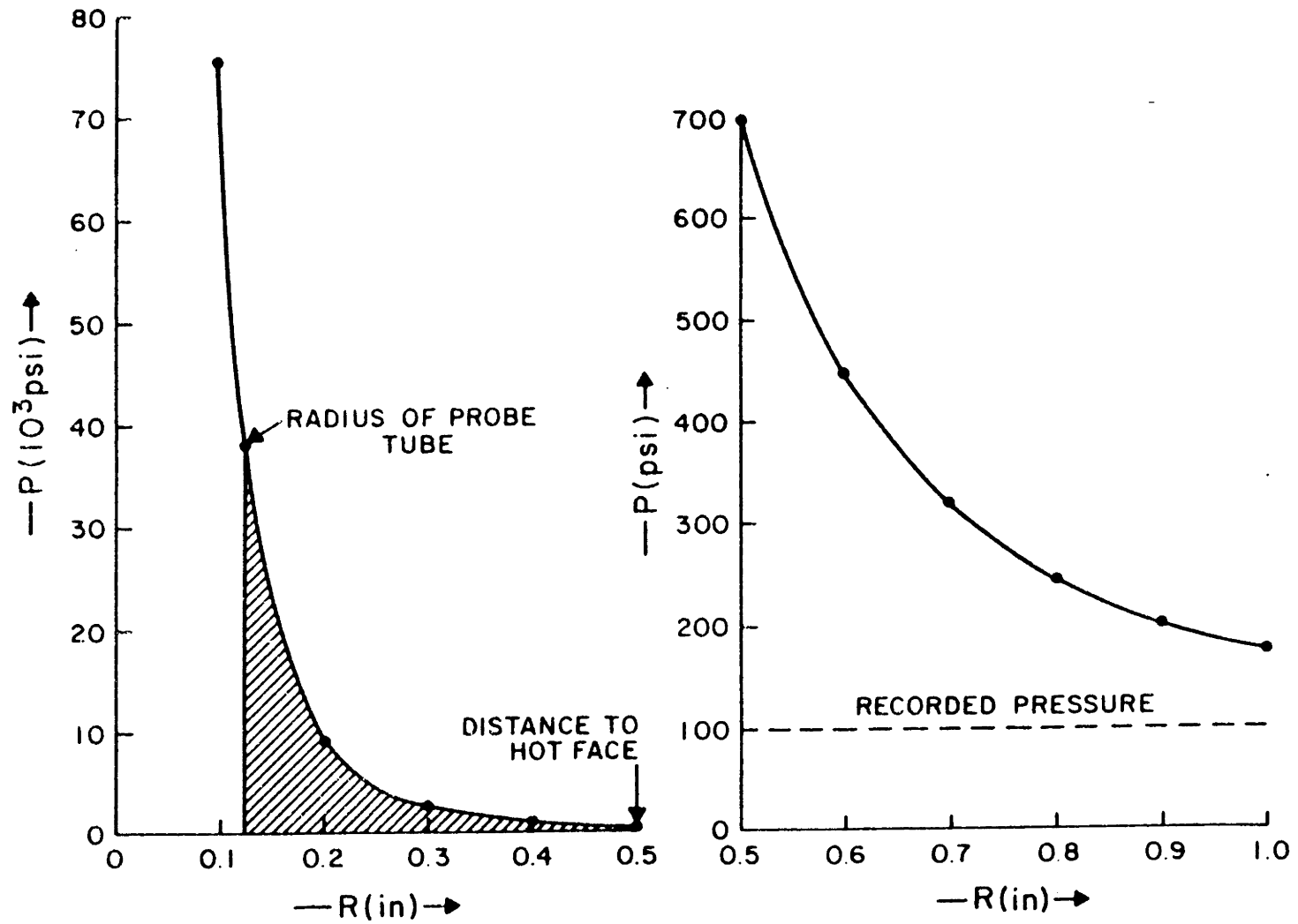


Fig. 10. In-pore steam pressure vs. radius of dehydrating spherical volume of castable having 10% bulk porosity.

To calculate theoretical steam pressures, water vapor is treated as an ideal gas such that $P_1V_1 = P_2V_2$ where P = pressure and V = volume. From this assumption, the following relationship is derived: $P(\text{recorded}) \times V(\text{instrument} + \text{castable sphere}) = P(\text{in-pore}) \times V(\text{castable sphere})$.

Two limits may be placed on this model. The first is that the largest sphere radius is the distance from the probe tube end to the hot face. Since probes at 0.5" from the hot face recorded levels of 100 psig (6.89 MPa), 0.5" is the probable upper end. The lowest possible radius is equal to that of the probe tube itself, 0.125". This places actual in-pore pressure at between 700 and 38,000 psig (48.2 and 2620 MPa) calculated from an instrument reading of 100 psig (6.89 MPa).

3. Factors Leading to Explosive Spalling

Critical zones for explosive spalling exist, and their locations are regulated by heat-up rate, permeability, and surface finish.

"Critical zones" for pressure build up parallel to the hot face are indicated by the sheet-like nature of spalled material. The plots of pressure maxima vs. depth for the 1000 and 1700^oF firings show a movement of critical zones from 1" to 1/2", respectively; with increased heating rate, steam pressures will build up much faster at

shallower depths. With more rapid pressure increase, material strength will be exceeded faster giving spalling at shallower depths from the hot face.

When initially heated, stresses are generated within the castable wall near the hot face. If heating rates increase, stresses build up closer to the hot face and critical zones for explosive spalling become shallower.

Castable permeability controls the rate at which internal steam pressure is allowed to dissipate. In dense concretes with low porosity, critical zones are closer to the hot face than those in more permeable materials. Surface finish of the hot face is also important. If the surface is cosmetically slicked, the surface will act as a vapor baffle and accelerate pressure build up. With faster increase in pressure, critical zones move to shallower depths.

VII. CONCLUSIONS

1. Internal steam pressures generated by castable dry-out can be easily and accurately measured by the new probe system.
2. Internal steam pressures may exceed 35,000 psi (2413 MPa).
3. Steam pressures are products of dehydration and changes in the cement phases.
4. Critical zones for explosive spalling exist, and their locations are regulated by heating rate, permeability and surface finish.
5. With use of internal pressure probes, heating schedules may be modified to reduce the occurrence of explosive spalling.

VIII. RECOMMENDATIONS

1. Further research must be conducted to determine critical zone depths for various castable compositions using normal heating schedules. Probes placed at these depths will then be able to warn of dangerous levels of internal steam pressure.
2. Castable dry-out heating schedules should be modified to reduce internal pressures. During initial heat-up, temperatures should be held just above the major dehydration points (212, 445-525, and 1022°F) to allow pressure to dissipate. Suggested temperatures are 300, 575, and 1050°F. Information gathered from pressure probes will determine how long temperatures must be held to allow pressure release.

IX. LITERATURE SOURCES

1. Carlson, E.T., "System Lime-Alumina-Water at 1C", J. Res. Nat. Bur. Std., 61 (1) 1-11 (1958).
2. Crowley, M.S., and Johnson, R.C., "Guidelines for Installing and Drying Refractory Concretes in Petrochemical Units", Am. Cer. Soc. Bull., 51 (3) 226-230 (1972).
3. Eusner, G.R., and Hubble, D.H., "Castable Technology", Am. Cer. Soc. Bull., 39 (8) 395-401 (1960).
4. Gitzen, W.H., and Hart, L.D., "Explosive Spalling of Castables", Am. Cer. Soc. Bull., 40 (7) 503-510 (1961).
5. Gitzen, W.H., Hart, L.D., and Maczura, G., "Properties of Some Calcium Aluminate Cement Compositions", J. Am. Cer. Soc., 40 (5) 158-167 (1957).
6. Givan, G.V., Hart, L.D., Heilich, R.P., and Maczura, G., "Curing and Firing High Purity Calcium Aluminate Bonded Tabular Alumina Castables", Presented at the Refractories Division Meeting of The American Ceramic Society, Bedford Springs, PA (1974).
7. Heindle, R.A., and Post, Z.A., "Refractory Castables: Preparation and some Properties", J. Am. Cer. Soc., 33 (7) 230-38 (1950).
8. Majumdar, A., and Roy, R., "The System $\text{CaO-Al}_2\text{O}_3\text{-H}_2\text{O}$ ", J. Am. Cer. Soc., 39 (12) 434-442 (1956).
9. Mehta, P.K., "Retrogression in the Hydraulic Strength of Calcium Aluminate Cement Structures," Miner. Process., 2 (11) 16-19 (1964).
10. Midgely, H.G., "The Mineralogy of Set High Aluminous Cement", Trans. Brit. Cer. Soc., 66 (4) 161-187 (1967).
11. Peppler, R.B., and Wells, L.S., "System of Lime, Alumina, and H_2O from 50C to 250C", J. Res. Nat. Bur. Std., 52 (2) 75-92 (1954).

12. Schneider, S.J., "Effect of Heat Treatment on the Constitution and Mechanical Properties of Some Hydrated Aluminous Cements", J. Am. Cer. Soc., 42 (4) 184-193 (1959).
13. Turriziani, B., "Calcium Aluminate Hydrates", in The Chemistry of Cement and Concrete, Vol. I (ed. H.F.W. Taylor), Academic Press, London, Eng., 233-286 (1964).
14. West, R.R., and Sutton, W. G., "Manufacture and Use of Fireclay Grog Refractories", Am. Cer. Soc. Bull., 30 (2) 34-40 (1951).
15. Wood, A.A.R., and Breibach, A.V., "The Effect of Curing Temperature on Strength of Castables", Trans. Brit. Cer. Soc., 64 (7) 333-349 (1965).
16. Wygant, J.F., and Crowley, M.S., "Curing Refractory Castables, It Isn't The Heat, It is The Humidity", Am. Cer. Soc. Bull., 43 (1) 1-5 (1964).
17. Yamamoto, et. al., "Drying and Explosive Spalling of Castable Refractories", Taikabutsu, 33, No. 283 23-27 (1981).

**The vita has been removed from
the scanned document**